J. Math. Fund. Sci., Vol. 48, No. 3, 2016, 241-251

Surface-to-volume Ratio of Synthesis Reactor Vessel Governing Low Temperature Crystallization of ZSM-5

Ana Hidayati Mukaromah[1], Grandprix Thomryes Marth Kadja[1],
Rino Rakhmata Mukti[1,2*], Ignatius Redyte Pratama[1],
Muhammad Ali Zulfikar[3] & Buchari[3]

[1]Division of Inorganic and Physical Chemistry,
Institut Teknologi Bandung, Jl. Ganesha 10, Bandung, 40132, Indonesia
[2]Research Center for Nanosciences and Nanotechnology,
Institut Teknologi Bandung, Jl. Ganesha 10, Bandung, 40132, Indonesia
[3]Division of Analytical Chemistry,
Institut Teknologi Bandung, Jl. Ganesha 10, Bandung, 40132, Indonesia
E-mail: rino@chem.itb.ac.id

Abstract. Zeolite ZSM-5 is one of the major catalysts in the petroleum and fine-chemical industries. The synthesis of zeolite ZSM-5 is usually carried out at a temperature above 100 °C using an immense amount of organic structure-directing agents (OSDA). It is interesting to note that fine-tuning the initial gel mixture can be used to enhance the typical slow crystallization rate of ZSM-5. Herein, we report the effect of the surface-to-volume ratio of the reactor vessel on the crystallization of ZSM-5 at low temperature. The surface-to-volume ratio of the reactor vessel influences the heat-transfer during the synthesis, which further governs the crystallization of ZSM-5. It was found that the higher the surface-to-volume of the reactor, the more crystalline the resulting product. The products with the highest crystallinity exhibited a nearly spherical morphology composed of smaller ZSM-5 crystallites. This phenomenon allows the presence of inter-crystallite mesopores, which is an advantage for the catalytic reaction of bulky molecules.

Keywords: *low OSDA; low temperature; mesopores; surface-to-volume ratio; ZSM-5.*

1 Introduction

Zeolite is a class of crystalline microporous (< 2 nm) aluminosilicate materials, arranged in a long-range order by TO4 (T = Si or Al) units. Zeolite is widely known for its application in particular fields such as sorption [1], catalysis [2,3] and ion-exchange [4]. Recently, its use has been extended to wider applications, including optical [5] and membrane technology [6]. Catalysis is the most known application of zeolite, for instance ZSM-5, especially for boosting the octane number in fluid catalytic cracking (FCC) units [7]. This is due to its peculiar structure comprising straight and zig-zag channels within sizes of around 5.5 Å and the presence of strong acid sites.

Received August 22nd, 2016, Revised October 13th, 2016, Accepted for publication December 8th, 2016.
ISSN: 2337-5760, DOI: 10.5614/j.math.fund.sci.2016.48.3.5

In general, the synthesis of ZSM-5 is conducted at high temperature (above 100 °C), which creates high autogenous pressure around 200-300 bar [8,9]. This kind of synthesis is actually undesired, due to the high energy consumption and the use of stainless-steel equipment, which requires safety handling. In addition, for synthesizing ZSM-5 one needs tetrapropylammonium bromide (TPABr) as the organic structure-directing agent (OSDA) in relatively large amounts to direct the crystallization of the ZSM-5 frameworks [10].

Recently, we have successfully realized the synthesis of ZSM-5 below 100 °C using a plastic bottle as reactor [11]. Decelerated crystallization as a consequence of lowering the temperature can be compensated using a dense gel system in which the concentration of each reactant is enhanced. In this composition, the amount of TPABr can be drastically reduced. Several parameters were varied to optimize the crystallization, including water ratio, Al content, NaOH concentration, and synergy of Na^+ and TPA^+ ions.

Apart from all of the abovementioned parameters, heat transfer is also important in the synthesis of inorganic materials including zeolite. Effective heat transfer may enhance the crystallization of zeolite [12]. Microwave synthesis and synthesis at ultrahigh temperatures have been used to provoke such effective heating. However, these strategies surely cannot be applied in our synthesis method. Therefore, an alternative strategy for effective heat transfer for synthesis of ZSM-5 at low temperature should be addressed. Bonaccorsi and Poverbio [12] reported the synthesis of NaA zeolite in two different reactors with a volume of 100 and 500 mL using microwave heating. They obtained more pure products by using the smaller reactor, which allows a better microwave penetration with more effective heat transfer. Okubo and his co-workers have shown that effective fast transfer can be realized using a stainless-steel tubular reactor with high surface-to-volume ratio [13]. Their strategy enables a significant enhancement of the crystallization rate of various microporous materials, such as SSZ-13 [14], ALPO-5 [13], Silicalite-1 [15], SAPO-AFI [16] and SAPO-CHA [16]. The fully crystalline products were obtained within a time scale of only 1 minute. However, it should be noted that all the above studies were performed at high temperature, i.e. above 150 °C. Lowering the temperature below 100 °C necessitates the substitution of the stainless-steel reactor by a low-cost plastic reactor, otherwise the high autogenous pressure cannot be created during synthesis.

In this contribution, we provide an investigation on the effect of the surface-to-volume ratio of the plastic reactor used in low-temperature synthesis of ZSM-5. Our present result suggests that the crystallization of ZSM-5 at low temperature is sensitive to the surface-to-volume ratio of the reactor vessel, which is likely to be correlated with the occurring heat transfer.

2 Experimental Section

2.1 Materials

The chemicals used in this study were Ludox HS-40 (colloidal silica, Sigma Aldrich), sodium aluminate ($NaAlO_2$, Sigma Aldrich), tetrapropylammonium bromide (TPABr, Sigma Aldrich), sodium hydroxide 50 %wt (NaOH, Merck) and demineralized water (H_2O). They were in reagent grade and used directly, without post-treatment.

2.2 Synthesis of ZSM-5 using Reactor Vessels with Different Surface-to-volume Ratios

$NaAlO_2$ and NaOH solution were mixed together in four plastic (polypropylene) bottles, i.e. reactors I, II, III and IV, with different surface-to-volume ratios serving as the synthesis reactor vessels, as illustrated in Figure 1. A stirred TPABr solution and Ludox HS-40 were then added to give a mixture with molar composition of 1 SiO_2: 0.005 Al_2O_3: 0.12 NaOH: 0.04 TPABr: 7.6 H_2O. The reactor vessel was sealed and vigorously stirred until a dense white gel was obtained. The total weight of the synthesis mixture was fixed at 35 gr. The synthesis mixture was subsequently transferred to an oven and heated at a temperature of 90 °C for 4 days. After the reaction, white solid products were obtained and quenched to ambient temperature. These products were separated, washed with deionized water, dried at 100 °C, and calcined at 550 °C for 6 hours.

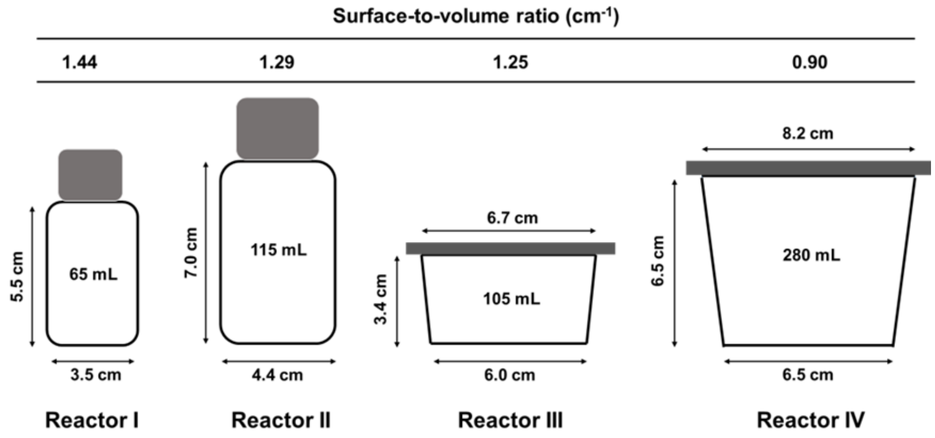

Figure 1 The reactor vessels with different surface-to-volume ratios used in the synthesis of ZSM-5 at low temperature.

2.3 Characterizations

X-ray diffraction (XRD) measurements were carried out on a Bruker D8 Discover using Cu-Kα (λ = 1.5418 Å) radiation to characterize the phase purity and crystallinity of the samples. The XRD patterns were collected at a 2θ angle of 3-5° with 0.02° intervals between each point. The crystallinity of each sample was derived by comparing the integrated area of the reflections at a 2θ angle of 22.5-25° with that of standard ZSM-5 sample possessing a perfect hexagonal-prismatic morphology, assuming 100% crystallinity (ASTM D5758-01 [17]). The crystallite size was calculated using the following Scherrer equation:

$$D = \frac{0.9\lambda}{\beta \cos\theta} \tag{1}$$

where, D = the crystalline size, λ = the X-ray wavelength, β = the full width at half maximum (FWHM), and θ = the Bragg angle.

The Fourier transform infrared (FTIR) spectra were measured on a Perkin Elmer 3100 spectrometer using the KBr pellet technique to identify the bonding vibration within the zeolite frameworks. The result from the FTIR measurement can be used to determine the ZSM-5 crystallinity by calculating the ratio between the bands at 550 $\mathrm{cm^{-1}}$ and 450 $\mathrm{cm^{-1}}$ [18]. The ratio between these bands for standard ZSM-5, assuming 100% crystallinity, is 0.806.

The morphology of the samples was observed using a scanning electron microscope (JEOL JSM 6510LV) operated at 5 kV.

The N_2 adsorption-desorption isotherms were measured in liquid N_2 medium at 77 K using a Quantachrome Autosorb iQ-MP instrument to determine the textural properties of the samples. Before measurement, each sample was outgassed at 300 °C for 6 h to remove the adsorbed water molecules, which may block the pores of the ZSM-5. The BET method was employed to determine the specific surface area (S_{BET}), while the t-plot method was used to calculate the micropore volume (V_{micro}) and the external surface area (S_{ext}). The total pore volume (V_{tot}) was obtained by measuring the amount of adsorbed nitrogen at a relative pressure (P/Po) of ca. 0.99. The mesopore volume was obtained by subtracting V_{tot} with V_{micro}. The non-localized density functional theory (NLDFT) model was used to determine the mesopore size distribution [19]. All textural properties were determined using the adsorption branch.

3 Results and Discussion

Crystallization of ZSM-5 at low temperature (90 ºC) was successfully achieved in 4 days. It should be noted that the TPABr used in this study was much lower than that of the typical syntheses with TPABr/Si ratio around 0.1-0.3 [10,20,21]. Figure 2(a) depicts the XRD patterns of the products from the different reactors. The products from reactors III and IV exhibited a bump around a 2θ angle of 15-35°, which is a characteristic feature of amorphous silica. Meanwhile, the products from reactors I and II displayed more intense reflections without observed amorphous bumps. Figure 2(b) shows a plot of the surface-to-volume ratio of the reactors versus the crystallinity obtained from the XRD data. We found a proportional relationship between the crystallinity and the surface-to-volume ratio of the reactor, in which the higher the surface-to-volume ratio of the reactor, the higher the crystallinity of the obtained products.

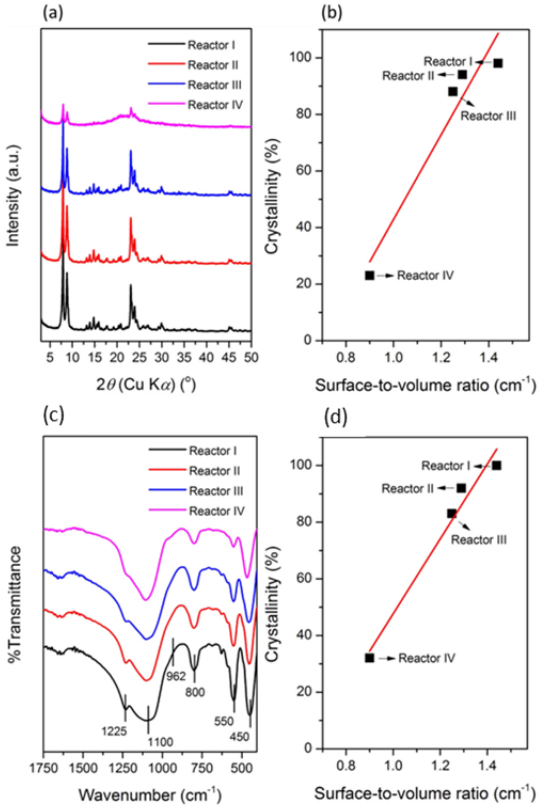

Figure 2 (a) XRD patterns and (b) plots of crystallinity derived from XRD pattern versus surface-to-volume ratio of the reactors, while (c) shows FTIR spectra of the products and (d) their plots of crystallinity versus surface-to-volume ratio of the reactors.

The FTIR spectra of the ZSM-5 samples are depicted in Figure 2(c). The information about the Si–O bonds is found in the wavenumber range from 1400 cm^{-1} to 400 cm^{-1}. The most intense band at 1100 cm^{-1} is attributed to the transversal mode of asymmetric stretching of Si–O–Si bonds. Another band at 1225 cm^{-1} corresponds to Si–O–Si asymmetric stretching vibration between SiO_4 tetrahedral, which is typical for zeolitic phases. The spectra of the products from reactor IV showed the least intense band at this wavenumber due to the significant presence of the amorphous part. Furthermore, a small shoulder at 962 cm^{-1} is attributed to the in-plane stretching vibration of Si–OH (silanol) bonds. The band at 800 cm^{-1} corresponds to the symmetric stretching vibration of Si–O–Si bonds and its bending vibration appears at 450 cm^{-1}. The band at 550 cm^{-1} corresponds to the asymmetric stretching vibration of the double five-membered rings (*d5r*) in the pentasil building units, which is a characteristic of ZSM-5 frameworks. The information about the crystallinity of the products was estimated by the intensity ratio between the bands at 550 cm^{-1} and 450 cm^{-1} [18]. All of the band assignments were in accordance with the previous literatures [22,23]. The order of the crystallinity showed a similarity compared to that of the XRD data, as shown in Figure 2(d). The results from the FTIR spectra support the insight that a reactor with a higher surface-to-volume ratio will result in higher crystalline products, as demonstrated by the XRD data. Reactors with a higher surface-to-volume ratio enhance the heat transfer. Presumably, a more effective heat transfer can induce nucleation more quickly since it is an energy-activated process, thus resulting in higher crystalline ZSM-5. It was clearly shown that the surface-to-volume ratio of the reactor governed the occurring crystallization of ZSM-5 below 100 °C.

It should be carefully noted that plastic material possesses lower thermal conductivity compared to that of stainless steel. Thus, the temperature increment rate that the inside part of a plastic reactor needs to reach the desired temperature is lower than that of a stainless-steel reactor. This merits further study to verify whether this temperature increment rate significantly influences the synthesis of ZSM-5 at low temperature. Nevertheless, it is interesting that not only high-temperature synthesis but also low-temperature synthesis of ZSM-5 is sensitive to the surface-to-volume ratio of the reactor. This provides a facile alternative way to control the crystallization of ZSM-5 at low temperature in addition to modifying the initial gel mixture or the synthesis conditions.

The products from reactor I were chosen to be further analyzed using SEM and an N_2 adsorption-desorption method, since it possessed the highest crystallinity of the four samples. Figures 3(a) and (b) show an SEM image of the products from reactor I. The observed morphology was nearly spherical, with a size of around 700 nm as calculated by the histogram in Figure 3(c). The calculated crystallite size using the Scherrer equation, Eq. (1), was 40 nm, suggesting that the observed particle was not a single particle but an aggregate composed of smaller ZSM-5 crystallites. Under low-temperature synthesis, a great number of nuclei may be formed resulting in nano-sized ZSM-5 crystallites. It has been previously reported that TPA^+ can act as a scaffolding agent to help assembling these nano-sized crystallites [11,24]. Furthermore, since the size of the crystallites is smaller than 1 µm, van der Waals interaction can be particularly significant to keep the crystallites together in an aggregate [25]. This occurrence may enable the presence of mesopores through the voids between the smaller crystallites.

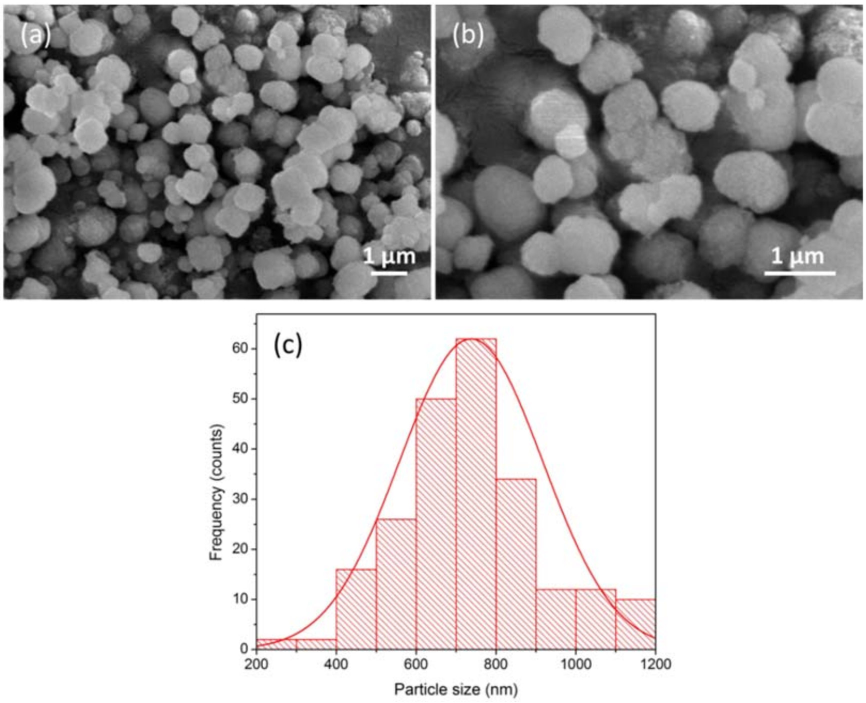

Figure 3 (a,b) SEM images of the products from reactor I and (c) the corresponding histogram showing the particle size distribution of the resulted ZSM-5.

Figure 4(a) shows the N_2 adsorption-desorption isotherm of the products from reactor I. As can be seen, the isotherm exhibited the IV-type hysteresis loop with a well-known step down at relative pressure (P/Po) around 0.42 [26]. This phenomenon indicates the occurring capillary condensation in meso-sized (2-50 nm) pores. The uptake rise at P/Po of 0.9-1.0 is an indication of inter-crystallite mesoporosity [27]. As calculated from the N_2 adsorption-desorption isotherm, the V_{micro} of the products from reactor I was 0.12 cm^3/g, showing well-defined microporosity within the zeolite framework. This was more evidence of the highly crystalline ZSM-5, as also demonstrated by the XRD and FTIR data. In addition, the products from reactor I possessed a large specific surface area (350 m^2/g) with 22.8% of it (80 m^2/g) a contribution from the external surface area of the mesopores. The NLDFT pore size distribution (Figure 4(b)) shows a peak at around 3.5 nm, which further confirms the presence of mesopores arisen from the inter-crystallite voids. Such development of mesoporosity with preserved mesoporosity may be useful in the catalytic reaction with bulky molecules acting as reactants.

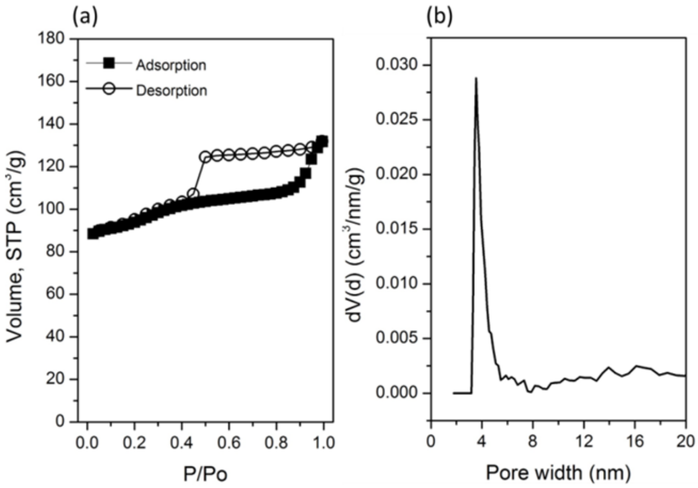

Figure 4 (a) N_2 adsorption-desorption isotherm of the products from reactor I and (b) the corresponding NLDFT pore size distribution.

4 Conclusion

In conclusion, crystallization of ZSM-5 at low temperature (90 °C) was successfully realized, even with a very low amount of TPABr. The course of crystallization is sensitive to the surface-to-volume ratio of the used plastic reactor due to the difference in heat transfer in each reactor. A more effective heat transfer may enhance the course of nucleation during the synthesis, which results in higher crystalline ZSM-5 products. The synthesized ZSM-5 exhibits the development of mesopores from inter-crystallite voids with preserved microporosity.

Acknowledgments

AHM thanks to the scholarship under the BPPDN program from the Ministry of Research, Technology and Higher Education (Kemenristekdikti) of the Republic of Indonesia. GTMK also thanks to Kemenristekdikti of the Republic of Indonesia for the PMDSU scholarship program. This work is supported by the ITB Research and Innovation Funding 2016.

References

[1] Zhao, Y-W., Shen, B-X., Sun, H., Zhan, G-X. & Liu, J-C., *Adsorption of Dimethyl Disulfide on ZSM-5 from Methyl Tert-butyl Ether Liquid: A Study on Equilibrium and Kinetics*, Fuel Process. Technol., **145**, pp. 14-19, 2016.

[2] Xue, Z., Zhang, T., Ma, J., Miao, H., Fan, W., Zhang, Y. & Li, R., *Accessibility and Catalysis of Acidic Sites in Hierarchical ZSM-5 Prepared by Silanization*, Microporous Mesoporous Mater., **151**, pp. 271-276, 2012.

[3] Miyake, K., Hirota, Y., Ono, K., Uchida, Y., Tanaka, S. & Nishiyama, N., *Direct and Selective Conversion of Methanol to Para-xylene over Zn Ion Doped ZSM-5/silicalite-1 Core-shell Zeolite Catalyst*, J. Catal., **342**, pp. 63-66, 2016.

[4] Abda, M.B., Schäf, O. & Zerega, Y., *Ion Exchange Effect on Asymmetric Dioxins Adsorption onto FAU-type X-zeolites*, Microporous Mesoporous Mater., **217**, pp. 178-183, 2015.

[5] Kim, H.S. & Yoon, K.B., *Preparation and Characterization of CdS and PbS Quantum Dots in Zeolite Y and their Applications for Nonlinear Optical Materials and Solar Cell*, Coord. Chem. Rev., **263-264**, pp. 239-256, 2014.

[6] Cai, X., Zhang, Y., Yin, L., Ding, D., Jing, W. & Gu, X., *Electrochemical Impedance Spectroscopy for Analyzing Microstructure Evolution of NaA Zeolite Membrane in Acid Water/ethanol Solution*, Chem. Eng. Sci., **153**, pp. 1-9, 2016.

[7] Viswanadham, N., Kamble, R., Saxena, S.K. & Singh, M., *Enhanced Octane Boosting Reactions of Light Naphtha on Mesoporous ZSM-5*, Catal. Commun., **9**, pp. 1894-1897, 2008.

[8] Cundy, C.S. & Cox, P.A., *The Hydrothermal Synthesis of Zeolites: History and Development from the Earliest Days to the Present Time*, Chem. Rev., **103**, pp. 663-701, 2003.

[9] Rabenau, A., *Hydrothermal Synthesis in Acid Solutions – A Review*, Advanced Ceramics III, Somiya, S., ed., Elsevier, pp. 163-179, 1990.

[10] Konno, H., Tago, T., Nakasaka, Y., Ohnaka, R., Nishimura, J. & Masuda, T., *Effectiveness of Nano-scale ZSM-5 Zeolite and Its Deactivation Mechanism on Catalytic Cracking of Representative Hydrocarbons of Naphtha*, Microporous Mesoporous Mater., **175**, pp. 25-33, 2013.

[11] Kadja, G.T.M., Mukti, R.R., Liu, Z., Rilyanti, M., Ismunandar, Marsih, I.N., Ogura, M., Wakihara, T. & Okubo, T., *Mesoporogen-free Synthesis*

of Hierarchically Porous ZSM-5 below 100 °C, Microporous Mesoporous Mater., **226**, pp. 344-352, 2016.

[12] Bonaccorsi, L. & Proverbio, E., *Microwave Assisted Crystallization of Zeolite A from Dense Gels*, J. Cryst. Growth, **247**, pp. 555-562, 2003.

[13] Liu, Z., Wakihara, T., Nishioka, D., Oshima, K., Takewaki, T. & Okubo, T., *One-minute Synthesis of Crystalline Microporous Aluminophosphate ($AlPO_4$-5) by Combining Fast Heating with a Seed-assisted Method*, Chem. Commun., **50**, pp. 2526-2528, 2014.

[14] Liu, Z., Wakihara, T., Oshima, K., Nishioka, D., Hotta, Y., Elangovan, S.P., Yunaba, Y., Yoshikawa, T., Chaikittisilp, W., Matsuo, T., Takewaki, T. & Okubo, T., *Widening Synthesis Bottlenecks: Realization of Ultrafast and Continuous-flow Synthesis of High-silica Zeolite SSZ-13 for NOx Removal*, Angew. Chem. Int. Ed., **54**, pp. 5683-5687, 2015.

[15] Liu, Z., Wakihara, T., Anand, C., Keoh, S.H., Nishioka, D., Hotta, Y., Matsuo, T., Takewaki, T. & Okubo, T., *Ultrafast Synthesis of Silicalite-1 using a Tubular Reactor with a Feature of Rapid Heating*, Microporous Mesoporous Mater., **223**, pp. 140-144, 2016.

[16] Liu, Z., Wakihara, T., Nomura, N., Matsuo, T., Anand, C., Elangovan, S.P., Yunaba, Y., Yoshikawa, T. & Okubo, T., *Ultrafast and Continuous Flow Synthesis of Silicoaluminophosphates*, Chem. Mater., **28**, pp. 4840-4847, 2016.

[17] American Society for Testing and Material, *Standard Test Method for Determination of Relative Crystallinity of Zeolite ZSM-5 by X-Ray Diffraction*, **D5758-01**, 2002.

[18] Shukla, D.B. & Pandya, V.P., *Estimation of Crystalline Phase in ZSM-5 Zeolites by Infrared Spectroscopy*, J. Chem. Tech. Biotechnol., **44**, pp. 147-154, 1989.

[19] Landers, J., Gor, G.Y. & Neimark, A.V., *Density Functional Theory for Characterization of Porous Materials*, Colloids Surf. A, **437**, pp. 3-32, 2013.

[20] Petushkov, A., Yoon, S. & Larsen, S.C., *Synthesis of Hierarchical Nanocrystalline ZSM-5 with Controlled Particle Size and Mesoporosity*, Micropororous Mesoporous Mater., **137**, pp. 92-100, 2011.

[21] Yokomori, Y. & Idaka, S., *The Structure of TPA-ZSM-5 with Si/Al=23*, Microporous Mesoporous Mater, **28**, pp. 405-413.

[22] Al-Oweini, R. & El-Rassy, H., *Synthesis and Characterization by FTIR Spectroscopy of Silica Aerogels Prepared using Several Si(OR)4 and R''Si(OR')3 precursors,* J. Mol. Struct., **919**, pp. 140-145, 2009.

[23] Figueiredo, A.L., Araujo, A.S., Linares, M., Peral, Á., García, R.A., Serrano, D.P. & Fernandes Jr., V.J., *Catalytic Cracking of LDPE Over Nanocrystalline HZSM-5 Zeolite Prepared by Seed-assisted Synthesis from an Organic-template-free System*, J. Anal. Appl. Pyrol., **117**, pp. 132-140, 2016.

[24] Wang, J., Groen, J.C., Yue, W., Zhou, W. & Coppens, M-O., *Single-template Synthesis of Zeolite ZSM-5 Composites with Tunable Mesoporosity*, Chem. Commun., **44**, pp. 4653-4655, 2007.

[25] Hartley, P.A., Parfitt, G.D. & Pollack, L.B., *The Role of the Van der Waals Force in the Agglomeration of Powders Containing Submicron Particles*, Powder Tech., **42**, pp. 35-46, 1985.

[26] Thommes, M., Kaneko, K., Neimark, A.V., Olivier, J.P., Rodriguez-Reinoso, F., Rouquerol, J. & Sing, K.S.W., *Physisorption of Gases, with Special Reference to the Evaluation of Surface Area and Pore Size Distribution (IUPAC Technical Report)*, Pure Appl. Chem., **87**, pp. 1051-1069, 2015.

[27] Taufiqurrahmi, N., Mohamed, A.R. & Bhatia, S., *Nanocrystalline Zeolite Beta and Zeolite Y as Catalyst in Used Palm Oil Cracking for the Production of Biofuel*, J. Nanopart. Res., **13**, pp. 3177-3189, 2011.